17th Australasian Fluid Mechanics Conference
Auckland, New Zealand
5-9 December 2010

Stability of plane-Poiseuille flow interacting with a finite compliant panel

M.W. Pitman[1] **and A.D. Lucey**[1]

[1]Fluid Dynamics Research Group
Curtin University of Technology, Perth, WA 6845, Australia

Abstract

This paper presents results from the application of a novel hybrid computational and theoretical technique to study the stability of a fluid-structure system that comprises fully developed plane Poiseuille flow at transitional Reynolds numbers over a finite flexible wall of streamwise extent. This builds upon our recent work [10] involving a uniform inviscid flow interacting with a flexible plate held at both its ends to include consideration of the full spatio-temporally evolving, rotational flow dynamics. Although presently considering the two-dimensional case the method may be extended to three-dimensions and arbitrary mean-flow fields other than plane Poiseuille.

Introduction

A numerical method is presented for the linear analysis of an incompressible, perturbed rotational flow at moderate Reynolds number interacting with a compliant surface. The linearised Navier-Stokes equations are used to represent the flow using a velocity-vorticity formulation that can accurately model perturbations without the need for turbulence models. This builds upon our recent work [10] involving a uniform inviscid flow interacting with a flexible plate held at both its ends to include consideration of the full spatio-temporally evolving, rotational flow dynamics.

In our modelling approach, we use the boundary-element method (BEM) - see [7] for details - along with an Eulerian formulation of the discrete vortex method (DVM) to determine the perturbations in the flow field due to wall motion. We loosely follow the approach of [4] who directly extracted the eigenmodes for fluid-based instabilities in laminar boundary-layer flow over a rigid wall. However, in our work, the flow field is modelled by the continuity equation and the linearised perturbation momentum equation written in velocity-vorticity form; this formulation is akin to that of [3]. The flow field is spatially discretised into rectangular elements on an Eulerian grid. A vector of flow-field element strengths is related to the values of a distributed vorticity field at control points through a matrix of influence coefficients. These influence matrices are evaluated computationally using an optimised fast multipole method (FMM) to overcome speed and memory limitations involved with the storage and evaluation of these large square matrix-vector products. An implicit restarted Arnoldi method based on Krylov subspace projections is then used to extract the eigenvalues and eigenvectors for the fully-coupled fluid-structure system from this very large set of linear equations.

A schematic of the flow-structure system is presented in Fig. 1. The rotational flow field that is studied in this case comprises a fully developed Poiseuille flow between two plates. A finite compliant section of the lower plate, of length L_C, interacts with the rotational flow field. The finite length compliant section is composed of a simple elastic plate which may have a uniformly distributed spring foundations and structural damping added. The system is similar to the configuration used by [1]. Although this work uses a Poiseuille mean flow profile, the robust computational method allows for the consideration of any mean flow profile and fluid-structure configuration.

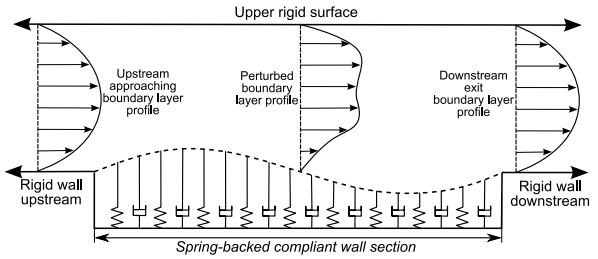

Figure 1: Schematic of the flow-structure system studied; the spring and dashpot foundations are absent for an unsupported elastic plate.

Background

Early work on compliant surfaces involved mainly analytical studies involving *infinite* compliant walls and inviscid, irrotational flow governed by Laplace's equation. In these cases, analytical solutions were obtained for the stability of the linearised flow-structure system, e.g. see the work of [2].

Subsequent investigation of finite compliant walls comprised numerical studies such as [7]. These studies adapted panel methods for the solution of Laplace's equation in the fluid domain, with the structural solution obtained using finite-difference methods. Coupling of fluid pressures and structural forces permitted solution of the strongly coupled flow-structure system through a time-stepping routine.

Carpenter & Davies [1] introduced a rotational flow field, solving the linearly perturbed flow field in velocity-vorticity form and then numerically coupling this to the structural solution. The solution of the coupled equations adopted a time-stepping method similar to [6] and therefore still produced results involving transient behaviour for a narrow set of initial or inlet conditions.

The use of Krylov subspace projection methods permit the extraction of eigenvalues and eigenvectors (modes) from large matrices. [4] analysed the linear spatio-temporal disturbance evolution in a boundary layer with rigid walls. This study also formulated the fluid equations (Navier-Stokes) in velocity-vorticity form. Using the same techniques for extraction of eigenvalues, [8] performed a similar linear analysis on an inviscid, finite-length, flow-structure compliant wall problem like that of [6].

The first coupling of a discrete-vortex method for a gridless velocity-vorticity solution method, to a non-linearly deforming compliant wall was performed by [9]. This method accounted for non-linear effects and gave DNS-type results for the coupled system through a time-stepping solution.

The present work employs a linearised variation of the velocity-

vorticity flow solution and coupling of [9] along with structural solution and eigenvalue extraction methods similar to [4]. The strongly coupled model can be used to analyse the spatio-temporal disturbance evolution and global stability of fluid-structure systems, giving a broader spectrum of stability information than practically available through the time-stepping solutions such as [1].

Computational Method

A description of the computational method is presented below. First, the equations and solution method for the fluid domain are considered. The structural solution and coupling of the system through the forcing pressure is then presented.

The equations are couched in finite difference form for the streamwise representation while Chebyshev differentiation matrices are used to evaluate the differential terms in the wall-normal direction. The use of mixed finite-difference and Chebyshev-differentiation matrices is more effective due to the high elemental aspect ratio, which suffers from numerical instability if finite difference representation alone is used in both directions.

Fluid domain

The flow field is modelled by the Navier-Stokes equations in linearised perturbation form as the continuity equation $\nabla.\vec{u}_p = 0$ and the linearised perturbation momentum equation

$$\left(\frac{\partial}{\partial t} + U\frac{\partial}{\partial x}\right)\vec{u}_p + v_p\frac{dU}{dy} = -\nabla p + \nu\left(\nabla^2\vec{u}_p\right) \quad , \qquad (1)$$

Eqn. 1 may be expressed in velocity-vorticity form with perturbation vorticity ω. Maintaining an Eulerian reference frame, and with mean-flow velocity profiles in the x and y directions denoted U and V respectively, this becomes

$$\frac{\partial\omega}{\partial t} + U\frac{\partial\omega}{\partial x} + u_p\frac{\partial\Omega}{\partial x} + V\frac{\partial\omega}{\partial y} + v_p\frac{\partial\Omega}{\partial y} = \nu\nabla^2\omega \ . \qquad (2)$$

This formulation is seen in the work of Davies & Carpenter [3]. For a plane parallel mean flow profile $V = 0$ and $U = f(y)$ and therefore $\frac{\partial\Omega}{\partial x} = 0$. In this case Eqn. 2 is reduced to

$$\frac{\partial\omega}{\partial t} + U\frac{\partial\omega}{\partial x} + v_p\frac{\partial\Omega}{\partial y} = \nu\nabla^2\omega \ . \qquad (3)$$

The flow field is spatially discretised into rectangular elements. The vorticity contained within each rectangular element is approximated by a zero-order vortex sheet element. A vector of flow field element strengths is defined as $\{\gamma\}$. These singularity element strengths are related to the distributed vorticity field as $\{\gamma\} = [H]\{\omega\}$, where $[H]$ is a matrix relating the distributed vorticity field at control points, $\{\omega\}$, to the singularity strengths. In this case, $[H]$ is a matrix consisting of only flow element thickness in the y-direction on the diagonal. Singularity elements which enforce the no-flux condition at the flow-structure interface are approximated by source(-sink) sheet elements, and a vector of wall element singularity strengths is defined as $\{\sigma\}$. The vector of y-direction perturbation velocities, v_p in Eqn. 3, at the flow elements is then

$$\left\{v_p\right\} = \left[I_{V,ff}\right]\{\gamma\} + \left[I_{V,wf}\right]\{\sigma\} \ . \qquad (4)$$

$\left[I_{A,bc}\right]$ is a matrix of coefficients that gives the A-velocity at the centres of elements b when multiplied with strengths of elements c. A may be either U for x-direction or V for y-direction velocity while b and c may be either f for fluid elements or w for wall elements.

The strength of the wall singularity strengths is determined through enforcing the no-flux boundary condition at the wall.

$$\{\sigma\} = \left[I_{V,ww}\right]^{-1}\left[D^+\right]\{\dot{\eta}\} - \left[I_{V,ww}\right]^{-1}\left[I_{V,fw}\right]\{\gamma\} \quad , \qquad (5)$$

where $\left[D^+\right]$ is a matrix which averages wall nodal velocities to give velocities at the wall panel centre points.

Substituting Eqn. 5 into Eqn. 4 gives the complete expression for y-direction perturbation velocity as

$$\left\{v_p\right\} = [A]\{\dot{\eta}\} + [B]\{\gamma\} \quad , \qquad (6)$$

where

$$[A] = \left[I_{V,wf}\right]\left[I_{V,ww}\right]^{-1}\left[D^+\right]$$
$$[B] = \left[\left[I_{V,ff}\right] - \left[I_{V,wf}\right]\left[I_{V,ww}\right]^{-1}\left[I_{V,fw}\right]\right] \ .$$

For the case of plane Poisueille flow that is considered here then $\frac{\partial\Omega}{\partial y} = -\frac{\partial U}{\partial y} = 2$. The vorticity gradient in the x-direction is calculated using a second-order-upwinding finite difference matrix such that $\{\dot{\omega}\} = \left[D_{F,1}\right]\{\omega\}$. Similarly, for the diffusive term second-order gradients in the x and y direction are handled using a centred finite difference and Chebychev differentiation matrices respectively. Eqn. 3 then may be expressed in discretised form as

$$[I]\{\dot{\omega}\} = [R]\{\omega\} - 2[A]\{\dot{\eta}\} \quad , \qquad (7)$$

where

$$[R] = \nu\left[D_{F,2}\right] + \nu\left[D_{C,2}\right] - [U]\left[D_{F,1}\right] - [B][H] \ .$$

Structural solution

The linear motion of the compliant wall is governed by the one-dimensional beam equation. Extra terms are added to account for the addition of a uniformly distributed spring foundation ($K\eta$) and uniform dashpot-type damping ($d\dot{\eta}$) to model the effects of energy dissipation in the wall structure.

$$\rho_m h\frac{\partial^2\eta}{\partial t^2} + d\frac{\partial\eta}{\partial t} + B\frac{\partial^4\eta}{\partial x^4} + K\eta = -\Delta p(x,0,t) \quad , \qquad (8)$$

where $\eta(x,t)$, ρ_m, h and B are, respectively, the plate's deflection, density, thickness and flexural rigidity, while $p(x,y,t)$ is the unsteady fluid pressure. In the present problem we apply hinged-edge conditions at the leading and trailing edges of the plate although in the method that follows there is no necessary restriction on such boundary conditions.

Eqn. 8 may be represented in discretised form as

$$\rho_m h[I]\{\ddot{\eta}\} + \Delta\{p\} = \left[-B\left[D_{F,4}\right] - K[I]\right]\{\eta\} - d[I]\{\dot{\eta}\} \ . \qquad (9)$$

Boundary Conditions

To implement the deterministic boundary conditions Eqn. 5 is modified to include calculation of the strengths of the flow elements that are closest to the wall in order to enforce the no-slip condition. The rate of vorticity injection is then expressed as an algebraic function of the other flow elements.

The perturbation flux and slip velocities at the wall elements are given respectively by:

$$\{n\} = \left[I_{V,ww}\right]\{\sigma\} + \left[I_{V,fw}\right]\{\gamma_w\} + \left[I_{V,fw}\right]\left\{\gamma_f\right\} - \{v_n\} \quad , \qquad (10)$$

$$\{t\} = \left[I_{U,ww}\right]\{\sigma\} + \left[I_{U,fw}\right]\{\gamma_w\} + \left[I_{U,fw}\right]\left\{\gamma_f\right\} \quad , \qquad (11)$$

where v_n is the velocity of the panel in the wall-normal direction which may be derived from the velocity at the nodes by $v_n = \left[D^+\right]\{\dot{\eta}\}$

By stating that the normal and tangential components of perturbation velocity must be equal to zero at the wall then the wall singularity strengths and near-wall fluid element strengths may then be solved *simultaneously* by solving the linear system of equations. Eqn. 11 gives an expression for the wall singularity elements and near-wall fluid singularity strengths in terms of remaining flow elements γ_f, these expressions may be summarized as:

$$\left\{ \begin{array}{c} \sigma \\ \omega_w \end{array} \right\} = \left[\begin{array}{cc} \left[S_{fw}\right]\left[H_f\right] & \left[S_w w\right] \\ \frac{1}{H_w}\left[S_{ff}\right]\left[H_f\right] & 0 \end{array} \right] \left\{ \begin{array}{c} \omega_f \\ \dot{\eta} \end{array} \right\} , \quad (12)$$

where H_w is the element thickness in the y-direction for fluid elements closest to the wall and $\left[H_f\right]$ is the diagonal-matrix of element thickness excluding near-wall flow elements and matrices $\left[S_{fw}\right]$ and $\left[S_{ff}\right]$ are the top and bottom halves of the matrix solution of the right-hand side of Eqn. 11 respectively.

This expression for wall strengths may be substituted for Eqn. 5 in the development of the fluid equations and the derivation of a fluid transport equation akin to Eqn. 7 may be derived. However it is necessary to replace the columns that correlate to the near-wall fluid elements in matrix $[R]$ of Eqn. 7 with the algebraic equivalents developed through Eqn. 12. The fluid elements, ω, in Eqn. 7 may be broken into near-wall and far-wall components ω_w and ω_f respectively and the equation may be re-phrased as

$$[I]\{\dot{\omega}\} = [R_w]\{\omega_w\} + \left[R_f\right]\left\{\omega_f\right\} - 2[A]\{\dot{\eta}\} \ . \quad (13)$$

Substituting Eqn. 12 into the first term of the right hand side of Eqn. 13 gives an expression for the vorticity transport in the discretised system as

$$[I]\left\{\dot{\omega}_f\right\} = [R_D]\left\{\omega_f\right\} - 2[A]\{\dot{\eta}\} \ . \quad (14)$$

where

$$[R_D] = \left[\frac{1}{H_w}[R_w]\left[S_{ff}\right]\left[H_f\right] + \left[R_f\right]\right]$$

Pressure Evaluation and Coupling

Through the Lighthill mechanism, described in [5] the pressure gradient along the wall is proportional to the rate of vorticity creation (or injection). Similarly, vorticity must be injected to at a rate that is equal to the generation of potential slip-velocity at the wall (through the no-slip boundary condition) so that

$$\rho \dot{u}_s = \rho \dot{\gamma}_w = -\frac{\partial p}{\partial s} \ . \quad (15)$$

The expression for $\dot{\gamma}_w$ may be derived from Eqn. 12 such that $\dot{\gamma}_w = [M_w]\left\{\dot{\Gamma}\right\}$ where $\{\Gamma\}$ is the time derivative of the vector of element strengths on the right hand side of Eqn. 12. In this case the perturbation pressure at the wall may be expressed as a numerical integral from the leading edge in matrix form as

$$\{\Delta p\} = [M_C]\left\{ \begin{array}{c} \dot{\omega}_f \\ \ddot{\eta} \end{array} \right\} , \quad (16)$$

where

$$[M_C] = \left[\Sigma_C^{\downarrow} dx\,[M_w]\right] , \quad (17)$$

and dx is the fluid element widths and $\left[\Sigma_C^{\downarrow}[M_w]\right]$ represents the cumulative sum of the rows of matrix $[M_w]$.

For a domain with periodic boundary conditions the pressure becomes an integral from the value at the upstream edge of the domain which may have an arbitrary value, therefore the pressure is normalised with respect to the average wall pressure to give

$$\{p\} = \left[[M_C] + \Sigma^{\downarrow}[M_C]\right]\left\{ \begin{array}{c} \dot{\omega}_f \\ \ddot{\eta} \end{array} \right\} , \quad (18)$$

where

$$[M_P] = \left[\left[[M_C] - \Sigma^{\downarrow}[M_C]\right]\right] , \quad (19)$$

and $\Sigma^{\downarrow}[M_C]$ represents the absolute sum of the columns of matrix $[M_C]$.

Results

Time-integration results

For the results presented below we use the dimensionless properties for the compliant wall that are defined in [1]. For dimensional reference, at a relatively high Reynolds number of 60000 this is dimensionally similar to air passing through a $2m$ wide channel with central velocity of $1m/s$. The compliant wall is dimensionally similar to very lightweight but stiff rubber-type material of $2mm$ thickness with a Young's modulus of $0.2GPa$ and density of $166kg/m^3$ on a very soft springy foundation of $0.53N/m^3$.

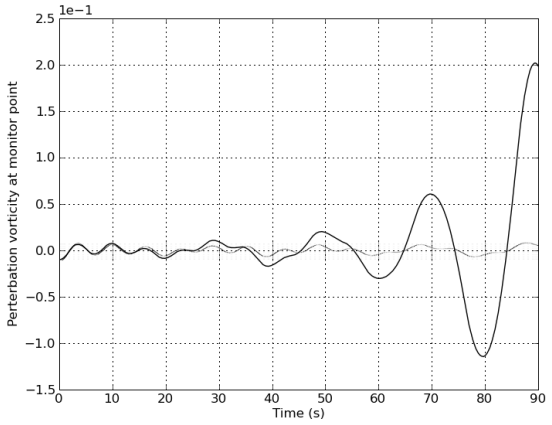

Figure 2: Plot of vorticity perterbation evolution at a monitor point located centre-channel at a downstream location of $x = 0.75L$ for the case of (feint line) a rigid channel and (bold line) a compliant insert at a Reynolds number of 6000.

Eigenvalue solution

Results are presented for the same system as that presented above except that the compliant wall properties are modified such that the finite flexible wall is of length $L_C = 6\,m$ centred on the lower boundary. The physical properties of the flexible wall are such that: thickness $h = 0.005\,m$, density $\rho = 1000\,kg/m^3$, Young's modulus $E = 2.592e7\,Pa$. Spring-backing is absent and a dashpot damping coefficient of $d = 10\,N.s/m$ is used.

The eigenvalue problem was solved for the rigid-wall system for a range of Reynolds numbers from $Re = 5000$ to 9000. The eigenvalues with largest real parts are plotted in Fig. 3. The results from this analysis indicate that instabilities (eigenvalues with positive real parts) begin to appear around $Re = 7200$. This

is in good agreement with the Orr-Sommerfeld relation which predicts the instability onset in a similar range of Reynolds numbers.

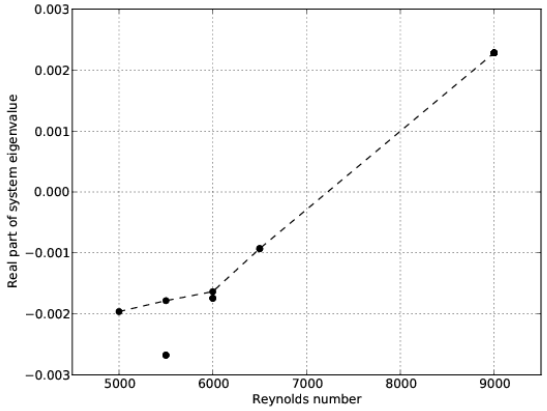

Figure 3: Real part of the system eigenvalues with largest real parts for reynolds numbers $Re = 5000,\ 5500,\ 6000,\ 6500$ and 9000 for channel flow with a rigid wall.

Figs. 4 show the eigenvector that corresponds to the eigenvalue solution with the largest real part (most unstable) at a Reynolds number of $Re = 6000$. The real part of the fluid-structure eigenvalue with largest real part is -1.698×10^{-3} which is approximately 4% lower than the rigid-wall case which has a value of -1.63×10^{-3}.

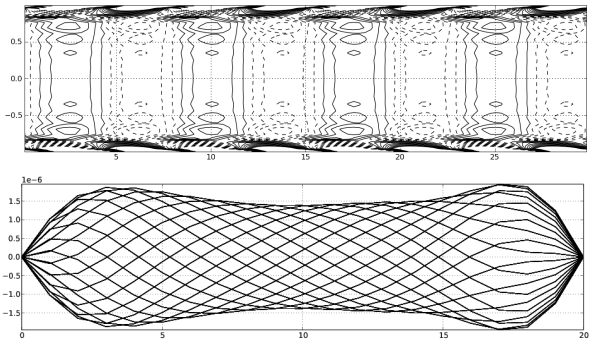

Figure 4: Contours of flow field vorticity (left) and wall modes (right) for a particular eigenmode of the flow-structure system at an instant in time at a Reynolds number of 6000.

Conclusions

This paper has presented a new solution method for the linear analysis of moderate Reynolds number flows interacting with a compliant surface. The preliminary results indicate that the computational method is robust and leaves a system of equations that are well-posed for linear analysis and eigenvalue extraction through Krylov subspace projection methods.

The system permits resolution of detailed two-dimensional flow phenomena at transitional Reynolds number with significantly fewer elements than would be required for a similar system model posed in primitive (u, v, p) variables. Initial results indicate that $N_y = 32$ Chebychev collocation points in the wall-normal direction and $N_x = 100$ finite difference node points in the streamwise direction are sufficient to resolve transitional flow phenomena at around $Re = 5000$ in a domain of channel height $L_y = 2\ m$ and length $L_x = 30\ m$. The results from this spatio-temporal model give good agreement with the Orr-Sommerfeld stability solution.

Investigation of the system eigenvalue solution both with and without a flexible panel present indicated that the addition of a flexible wall with structural damping improved global system stability by approximately 4% at a Reynolds number of $Re = 6000$. This indicates that the addition of periodically-spaced finite compliant walls with structural damping may be able to delay the onset of instabilities to higher Reynolds numbers. Results using the compliant wall properties of [1] resulted in a significant deterioriation of system stability. The reasons for this discrepancy in modelled outcomes is left for future work.

Acknowledgements

We would like to acknowledge the cooperation of the Fluid Dynamics Research Centre (FDRC) at Warwick University, UK. This research is supported by the Australian Research Council (ARC) through the Discovery Projects scheme.

References

[1] Carpenter, P. W. and Davies, C., Numerical simulation of the evolution of tollmien-schlichting waves over finite compliant surfaces, *Journal of Fluid Mechanics*, **335**, 1997, 361–392.

[2] Carpenter, P. W. and Garrad, A. D., The hydrodynamic stability of flows over kramer-type compliant coatings. part 1. tollmien-schlichting instabilities, *Journal of Fluid Mechanics*, **155**, 1985, 465–510.

[3] Davies, C. and Carpenter, P. W., A novel velocity-vorticity formulation of the navier-stokes equations with applications to boundary layer disturbance evolution, *Journal of Computational Physics*, **172**, 2001, 119–165.

[4] Ehrenstein, U. and Gallaire, F., On two-dimensional temporal modes in spatially evolving open flows: the flat-plate boundary layer., *Journal of Fluid Mechanics*, **536**, 2005, 209–218.

[5] Leonard, A., Vortex methods for flow simulation, *Journal of Computational Physics*, **37(3)**, 1980, 289–335.

[6] Lucey, A. D., Cafolla, G. J., Carpenter, P. W. and Yang, M., The nonlinear hydroelastic behaviour of flexible walls., *Journal of Fluids and Structures*, **11**, 1997, 717–744.

[7] Lucey, A. D. and Carpenter, P. W., A numerical simulation of the interaction of a compliant wall and an inviscid flow., *Journal of Fluid Mechanics*, **234**, 1992, 121–146.

[8] Lucey, A. D. and Pitman, M. W., A new method for determining the eigenmodes of finite flow-structure systems., in *ASME-PVP 2006: 2006 ASME Pressure Vessels and Piping Division Conference, Paper no. pvp2006-icpv11-93938*, 2006.

[9] Pitman, M. W. and Lucey, A. D., *Eigen-analysis of a fully viscous boundary-layer flow interacting with a finite compliant surface.*, Proc. of the 16th Australasian Fluid Mechanics Conference, 2nd-7th December 2007, Gold Coast, Australia, 2007.

[10] Pitman, M. W. and Lucey, A. D., On the direct determination of the eigenmodes of finite flow–structure systems, *Proceedings of the Royal Society A*, **465**, 2009, 257–281.